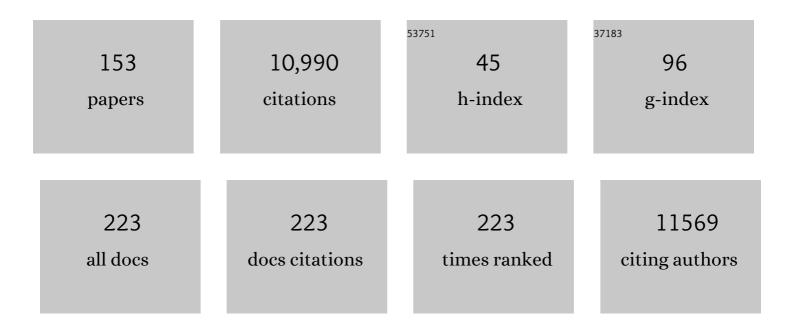
List of Publications by Year in descending order

Source: https://exaly.com/author-pdf/335352/publications.pdf Version: 2024-02-01



#	Article	IF	CITATIONS
1	Chlorine partitioning in the stratosphere based on in situ measurements. Tellus, Series B: Chemical and Physical Meteorology, 2022, 52, 934.	0.8	5
2	Analysis of atmospheric CO <sub>2</sub> growth rates at Mauna Loa using CO <sub>2</sub> fluxes derived from an inverse model. Tellus, Series B: Chemical and Physical Meteorology, 2022, 57, 357.	0.8	28
3	Variations of tropospheric methane over Japan during 1988–2010. Tellus, Series B: Chemical and Physical Meteorology, 2022, 66, 23837.	0.8	14
4	Seasonal and short-term variations in atmospheric potential oxygen at Ny-Ã…lesund, Svalbard. Tellus, Series B: Chemical and Physical Meteorology, 2022, 69, 1311767.	0.8	8
5	Regional trends and drivers of the global methane budget. Global Change Biology, 2022, 28, 182-200.	4.2	56
6	Effect of recent observations on Asian CO <sub>2</sub> flux estimates by transport model inversions. Tellus, Series B: Chemical and Physical Meteorology, 2022, 55, 522.	0.8	16
7	Sensitivity of optimal extension of CO <sub>2</sub> observation networks to model transport. Tellus, Series B: Chemical and Physical Meteorology, 2022, 55, 498.	0.8	8
8	Anthropogenic emission is the main contributor to the rise of atmospheric methane during 1993–2017. National Science Review, 2022, 9, nwab200.	4.6	20
9	Are Landâ€Use Change Emissions in Southeast Asia Decreasing or Increasing?. Global Biogeochemical Cycles, 2022, 36, .	1.9	7
10	Forward and Inverse Modelling of Atmospheric Nitrous Oxide Using MIROC4-Atmospheric Chemistry-Transport Model. Journal of the Meteorological Society of Japan, 2022, 100, 361-386.	0.7	8
11	Spatio-temporal variability of XCO2 over Indian region inferred from Orbiting Carbon Observatory (OCO-2) satellite and Chemistry Transport Model. Atmospheric Research, 2022, 269, 106044.	1.8	13
12	Seasonal and annual variations of CO2 and CH4 at Shadnagar, a semi-urban site. Science of the Total Environment, 2022, 819, 153114.	3.9	15
13	Definitions and methods to estimate regional land carbon fluxes for the second phase of the REgional Carbon Cycle Assessment and Processes Project (RECCAP-2). Geoscientific Model Development, 2022, 15, 1289-1316.	1.3	34
14	Applications of top-down methods to anthropogenic GHG emission estimation. , 2022, , 455-481.		0
15	Top-down approaches. , 2022, , 87-155.		0
16	Impact of Changing Winds on the Mauna Loa CO <sub>2</sub> Seasonal Cycle in Relation to the Pacific Decadal Oscillation. Journal of Geophysical Research D: Atmospheres, 2022, 127, .	1.2	3
17	Methane sources from waste and natural gas sectors detected in Pune, India, by concentration and isotopic analysis. Science of the Total Environment, 2022, 842, 156721.	3.9	3
18	An Analysis of Interhemispheric Transport Pathways Based on Threeâ€Đimensional Methane Data by GOSAT Observations and Model Simulations. Journal of Geophysical Research D: Atmospheres, 2022, 127, .	1.2	5

#	Article	IF	CITATIONS
19	Estimated regional CO <sub>2</sub> flux and uncertainty based on an ensemble of atmospheric CO <sub>2</sub> inversions. Atmospheric Chemistry and Physics, 2022, 22, 9215-9243.	1.9	22
20	Empirical estimates of regional carbon budgets imply reduced global soil heterotrophic respiration. National Science Review, 2021, 8, nwaa145.	4.6	70
21	Spatio-temporal variations of the atmospheric greenhouse gases and their sources and sinks in the Arctic region. Polar Science, 2021, 27, 100553.	0.5	6
22	Gridded fossil CO2 emissions and related O2 combustion consistent with national inventories 1959–2018. Scientific Data, 2021, 8, 2.	2.4	56
23	Emissions from the Oil and Gas Sectors, Coal Mining and Ruminant Farming Drive Methane Growth over the Past Three Decades. Journal of the Meteorological Society of Japan, 2021, 99, 309-337.	0.7	38
24	Seasonal Variations of SF <sub>6</sub> , CO <sub>2</sub> , CH <sub>4</sub> , and N <sub>2</sub> O in the UT/LS Region due to Emissions, Transport, and Chemistry. Journal of Geophysical Research D: Atmospheres, 2021, 126, e2020JD033541.	1.2	13
25	Methyl Chloroform Continues to Constrain the Hydroxyl (OH) Variability in the Troposphere. Journal of Geophysical Research D: Atmospheres, 2021, 126, e2020JD033862.	1.2	21
26	A three-dimensional-model inversion of methyl chloroform to constrain the atmospheric oxidative capacity. Atmospheric Chemistry and Physics, 2021, 21, 4809-4824.	1.9	13
27	GOSAT CH4 Vertical Profiles over the Indian Subcontinent: Effect of a Priori and Averaging Kernels for Climate Applications. Remote Sensing, 2021, 13, 1677.	1.8	4
28	Evaluation of earth system model and atmospheric inversion using total column CO2 observations from GOSAT and OCO-2. Progress in Earth and Planetary Science, 2021, 8, .	1.1	10
29	Nitrogen oxides concentration and emission change detection during COVID-19 restrictions in North India. Scientific Reports, 2021, 11, 9800.	1.6	29
30	New approach to evaluate satellite-derived XCO <sub>2</sub> over oceans by integrating ship and aircraft observations. Atmospheric Chemistry and Physics, 2021, 21, 8255-8271.	1.9	8
31	The consolidated European synthesis of CH <sub>4</sub> and N <sub>2</sub> O emissions for the European Union and United Kingdom: 1990–2017. Earth System Science Data, 2021, 13, 2307-2362.	3.7	16
32	Recent Slowdown of Anthropogenic Methane Emissions in China Driven by Stabilized Coal Production. Environmental Science and Technology Letters, 2021, 8, 739-746.	3.9	25
33	The Monitoring Nitrous Oxide Sources (MIN2OS) satellite project. Remote Sensing of Environment, 2021, 266, 112688.	4.6	8
34	Aerosol Loading and Radiation Budget Perturbations in Densely Populated and Highly Polluted Indoâ€Gangetic Plain by COVIDâ€19: Influences on Cloud Properties and Air Temperature. Geophysical Research Letters, 2021, 48, e2021GL093796.	1.5	14
35	Measurement report: Regional characteristics of seasonal and long-term variations in greenhouse gases at Nainital, India, and Comilla, Bangladesh. Atmospheric Chemistry and Physics, 2021, 21, 16427-16452.	1.9	10
36	Strong Southern Ocean carbon uptake evident in airborne observations. Science, 2021, 374, 1275-1280.	6.0	44

#	Article	IF	CITATIONS
37	Multispecies Assessment of Factors Influencing Regional CO <sub>2</sub> and CH <sub>4</sub> Enhancements During the Winter 2017 ACTâ€America Campaign. Journal of Geophysical Research D: Atmospheres, 2020, 125, e2019JD031339.	1.2	23
38	State of the science in reconciling topâ€down and bottomâ€up approaches for terrestrial CO <sub>2</sub> budget. Global Change Biology, 2020, 26, 1068-1084.	4.2	43
39	A comprehensive quantification of global nitrous oxide sources and sinks. Nature, 2020, 586, 248-256.	13.7	814
40	Detection of fossil-fuel CO2Âplummet in China due to COVID-19 by observation at Hateruma. Scientific Reports, 2020, 10, 18688.	1.6	22
41	PM2.5 diminution and haze events over Delhi during the COVID-19 lockdown period: an interplay between the baseline pollution and meteorology. Scientific Reports, 2020, 10, 13442.	1.6	75
42	Assessment of spatio-temporal distribution of CO2 over greater Asia using the WRF–CO2 model. Journal of Earth System Science, 2020, 129, 1.	0.6	8
43	Sources of Uncertainty in Regional and Global Terrestrial CO <sub>2</sub> Exchange Estimates. Global Biogeochemical Cycles, 2020, 34, e2019GB006393.	1.9	59
44	Can Delhi's Pollution be Affected by Crop Fires in the Punjab Region?. Scientific Online Letters on the Atmosphere, 2020, 16, 86-91.	0.6	16
45	The Global Methane Budget 2000–2017. Earth System Science Data, 2020, 12, 1561-1623.	3.7	1,199
46	Evaluating Simulations of Interhemispheric Transport: Interhemispheric Exchange Time Versus SF <sub>6</sub> Age. Geophysical Research Letters, 2019, 46, 1113-1120.	1.5	12
47	Global atmospheric CO <sub>2</sub> inverse models converging on neutral tropical land exchange, but disagreeing on fossil fuel and atmospheric growth rate. Biogeosciences, 2019, 16, 117-134.	1.3	77
48	A segmentation algorithm for characterizing rise and fall segments in seasonal cycles: an application to XCO <sub>2</sub> to estimate benchmarks and assess model bias. Atmospheric Measurement Techniques, 2019, 12, 2611-2629.	1.2	7
49	Assessing Lagrangian inverse modelling of urban anthropogenic CO2 fluxes using in situ aircraft and ground-based measurements in the Tokyo area. Carbon Balance and Management, 2019, 14, 6.	1.4	14
50	Acceleration of global N2O emissions seen from two decades of atmospheric inversion. Nature Climate Change, 2019, 9, 993-998.	8.1	229
51	The severe Delhi SMOG of 2016: A case of delayed crop residue burning, coincident firecracker emissions, and atypical meteorology. Atmospheric Pollution Research, 2019, 10, 868-879.	1.8	59
52	Plant Regrowth as a Driver of Recent Enhancement of Terrestrial CO <sub>2</sub> Uptake. Geophysical Research Letters, 2018, 45, 4820-4830.	1.5	32
53	Land use change and El Niño-Southern Oscillation drive decadal carbon balance shifts in Southeast Asia. Nature Communications, 2018, 9, 1154.	5.8	28
54	Methane and nitrous oxide emissions from conventional and modified rice cultivation systems in South India. Agriculture, Ecosystems and Environment, 2018, 252, 148-158.	2.5	88

#	Article	IF	CITATIONS
55	Age of air as a diagnostic for transport timescales in global models. Geoscientific Model Development, 2018, 11, 3109-3130.	1.3	44
56	The impact of transport model differences on CO <sub>2</sub> surface flux estimates from OCO-2 retrievals of column average CO <sub>2</sub> . Atmospheric Chemistry and Physics, 2018, 18, 7189-7215.	1.9	70
57	Temporal Variations of the Mole Fraction, Carbon, and Hydrogen Isotope Ratios of Atmospheric Methane in the Hudson Bay Lowlands, Canada. Journal of Geophysical Research D: Atmospheres, 2018, 123, 4695-4711.	1.2	13
58	Improved Chemical Tracer Simulation by MIROC4.0-based Atmospheric Chemistry-Transport Model (MIROC4-ACTM). Scientific Online Letters on the Atmosphere, 2018, 14, 91-96.	0.6	50
59	Global Carbon Budget 2018. Earth System Science Data, 2018, 10, 2141-2194.	3.7	1,167
60	U.S. CH <sub>4</sub> emissions from oil and gas production: Have recent large increases been detected?. Journal of Geophysical Research D: Atmospheres, 2017, 122, 4070-4083.	1.2	47
61	The Orbiting Carbon Observatory (OCO-2) tracks 2–3 peta-gram increase in carbon release to the atmosphere during the 2014–2016 El Niño. Scientific Reports, 2017, 7, 13567.	1.6	35
62	Temporal Characteristics of CH <sub>4</sub> Vertical Profiles Observed in the West Siberian Lowland Over Surgut From 1993 to 2015 and Novosibirsk From 1997 to 2015. Journal of Geophysical Research D: Atmospheres, 2017, 122, 11,261.	1.2	12
63	Implications of overestimated anthropogenic CO2 emissions on East Asian and global land CO2 flux inversion. Geoscience Letters, 2017, 4, .	1.3	44
64	Reconciliation of top-down and bottom-up CO <sub>2</sub> fluxes in Siberian larch forest. Environmental Research Letters, 2017, 12, 125012.	2.2	13
65	What controls the seasonal cycle of columnar methane observed by GOSAT over different regions in India?. Atmospheric Chemistry and Physics, 2017, 17, 12633-12643.	1.9	26
66	Variability and quasi-decadal changes in the methane budget over the period 2000–2012. Atmospheric Chemistry and Physics, 2017, 17, 11135-11161.	1.9	85
67	Global inverse modeling of CH <sub>4</sub> sources and sinks: an overview of methods. Atmospheric Chemistry and Physics, 2017, 17, 235-256.	1.9	75
68	Evaluation of column-averaged methane in models and TCCON with a focus on the stratosphere. Atmospheric Measurement Techniques, 2016, 9, 4843-4859.	1.2	23
69	The terrestrial carbon budget of South and Southeast Asia. Environmental Research Letters, 2016, 11, 105006.	2.2	39
70	Regional carbon fluxes from land use and land cover change in Asia, 1980–2009. Environmental Research Letters, 2016, 11, 074011.	2.2	31
71	A multi-model intercomparison of halogenated very short-lived substances (TransCom-VSLS): linking oceanic emissions and tropospheric transport for a reconciled estimate of the stratospheric source gas injection of bromine. Atmospheric Chemistry and Physics, 2016, 16, 9163-9187.	1.9	51
72	Temporal variations of atmospheric CO <sub>2</sub> and CO at Ahmedabad in western India. Atmospheric Chemistry and Physics, 2016, 16, 6153-6173.	1.9	51

#	Article	IF	CITATIONS
73	Increasing summer net CO <sub>2</sub> uptake in high northern ecosystems inferred from atmospheric inversions and comparisons to remote-sensing NDVI. Atmospheric Chemistry and Physics, 2016, 16, 9047-9066.	1.9	33
74	Regional Methane Emission Estimation Based on Observed Atmospheric Concentrations (2002-2012). Journal of the Meteorological Society of Japan, 2016, 94, 91-113.	0.7	55
75	Top–down assessment of the Asian carbon budget since the mid 1990s. Nature Communications, 2016, 7, 10724.	5.8	93
76	Simulation of CO 2 concentrations at Tsukuba tall tower using WRF-CO 2 tracer transport model. Journal of Earth System Science, 2016, 125, 47-64.	0.6	10
77	The global methane budget 2000–2012. Earth System Science Data, 2016, 8, 697-751.	3.7	824
78	Variations in global methane sources and sinks during 1910–2010. Atmospheric Chemistry and Physics, 2015, 15, 2595-2612.	1.9	108
79	Air–sea CO <sub>2</sub> flux in the Pacific Ocean for the period 1990–2009. Biogeosciences, 2014, 11, 709-734.	1.3	68
80	Global emissions of refrigerants HCFC-22 and HFC-134a: Unforeseen seasonal contributions. Proceedings of the National Academy of Sciences of the United States of America, 2014, 111, 17379-17384.	3.3	59
81	Observational evidence for interhemispheric hydroxyl-radical parity. Nature, 2014, 513, 219-223.	13.7	121
82	Retrieval of nitrous oxide from Atmospheric Infrared Sounder: Characterization and validation. Journal of Geophysical Research D: Atmospheres, 2014, 119, 9107-9122.	1.2	21
83	TransCom N <sub>2</sub> O model inter-comparison – Part 1: Assessing the influence of transport and surface fluxes on tropospheric N <sub>2</sub> O variability. Atmospheric Chemistry and Physics, 2014, 14, 4349-4368.	1.9	34
84	Global and regional emissions estimates for N <sub>2</sub> O. Atmospheric Chemistry and Physics, 2014, 14, 4617-4641.	1.9	91
85	TransCom N <sub>2</sub> O model inter-comparison – Part 2: Atmospheric inversion estimates of N <sub>2</sub> O emissions. Atmospheric Chemistry and Physics, 2014, 14, 6177-6194.	1.9	49
86	Enhanced Seasonal Exchange of CO <sub>2</sub> by Northern Ecosystems Since 1960. Science, 2013, 341, 1085-1089.	6.0	329
87	On the variation of regional CO <sub>2</sub> exchange over temperate and boreal North America. Global Biogeochemical Cycles, 2013, 27, 991-1000.	1.9	10
88	First intercalibration of column-averaged methane from the Total Carbon Column Observing Network and the Network for the Detection of Atmospheric Composition Change. Atmospheric Measurement Techniques, 2013, 6, 397-418.	1.2	24
89	Impact of transport model errors on the global and regional methane emissions estimated by inverse modelling. Atmospheric Chemistry and Physics, 2013, 13, 9917-9937.	1.9	68
90	Off-line algorithm for calculation of vertical tracer transport in the troposphere due to deep convection. Atmospheric Chemistry and Physics, 2013, 13, 1093-1114.	1.9	27

#	Article	IF	CITATIONS
91	Atmospheric column-averaged mole fractions of carbon dioxide at 53 aircraft measurement sites. Atmospheric Chemistry and Physics, 2013, 13, 5265-5275.	1.9	20
92	Corrigendum to "Atmospheric column-averaged mole fractions of carbon dioxide at 53 aircraft measurement sites" published in Atmos. Chem. Phys. 13, 5265–5275, 2013. Atmospheric Chemistry and Physics, 2013, 13, 9213-9216.	1.9	2
93	Validation of XCO <sub>2</sub> derived from SWIR spectra of GOSAT TANSO-FTS with aircraft measurement data. Atmospheric Chemistry and Physics, 2013, 13, 9771-9788.	1.9	106
94	TransCom model simulations of methane: Comparison of vertical profiles with aircraft measurements. Journal of Geophysical Research D: Atmospheres, 2013, 118, 3891-3904.	1.2	24
95	The carbon budget of South Asia. Biogeosciences, 2013, 10, 513-527.	1.3	94
96	Global atmospheric carbon budget: results from an ensemble of atmospheric CO <sub>2</sub> inversions. Biogeosciences, 2013, 10, 6699-6720.	1.3	356
97	Sea–air CO <sub>2</sub> fluxes in the Indian Ocean between 1990 and 2009. Biogeosciences, 2013, 10, 7035-7052.	1.3	47
98	Carbon and hydrogen isotopic ratios of atmospheric methane in the upper troposphere over the Western Pacific. Atmospheric Chemistry and Physics, 2012, 12, 8095-8113.	1.9	30
99	Technical Note: Latitude-time variations of atmospheric column-average dry air mole fractions of CO <sub>2</sub> , CH <sub>4</sub> and N <sub>2</sub> O. Atmospheric Chemistry and Physics, 2012, 12, 7767-7777.	1.9	25
100	Iconic CO <sub>2</sub> Time Series at Risk. Science, 2012, 337, 1038-1040.	6.0	15
101	The rapidly changing greenhouse gas budget of Asia. Eos, 2012, 93, 237-237.	0.1	8
102	Distribution of methane in the tropical upper troposphere measured by CARIBIC and CONTRAIL aircraft. Journal of Geophysical Research, 2012, 117, .	3.3	38
103	Simulation of CO <sub>2</sub> Concentration over East Asia Using the Regional Transport Model WRF-CO <sub>2</sub> . Journal of the Meteorological Society of Japan, 2012, 90, 959-976.	0.7	24
104	Atmospheric CO <sub>2</sub> inversion validation using vertical profile measurements: Analysis of four independent inversion models. Journal of Geophysical Research, 2011, 116, .	3.3	41
105	Assessing the impact of satellite, aircraft, and surface observations on CO2flux estimation using an ensemble-based 4-D data assimilation system. Journal of Geophysical Research, 2011, 116, .	3.3	20
106	Tropospheric distribution and variability of N <sub>2</sub> O: Evidence for strong tropical emissions. Geophysical Research Letters, 2011, 38, .	1.5	78
107	TransCom satellite intercomparison experiment: Construction of a bias corrected atmospheric CO <sub>2</sub> climatology. Journal of Geophysical Research, 2011, 116, .	3.3	19
108	TransCom model simulations of CH <sub>4</sub> and related species: linking transport, surface flux and chemical loss with CH <sub>4</sub> variability in the troposphere and lower stratosphere. Atmospheric Chemistry and Physics, 2011, 11, 12813-12837.	1.9	331

7

#	Article	IF	CITATIONS
109	TransCom continuous experiment: comparison of <sup>222</sup> Rn transport at hourly time scales at three stations in Germany. Atmospheric Chemistry and Physics, 2011, 11, 10071-10084.	1.9	25
110	Carbon balance of South Asia constrained by passenger aircraft CO <sub>2</sub> measurements. Atmospheric Chemistry and Physics, 2011, 11, 4163-4175.	1.9	78
111	Three-dimensional variations of atmospheric CO <sub>2</sub> : aircraft measurements and multi-transport model simulations. Atmospheric Chemistry and Physics, 2011, 11, 13359-13375.	1.9	41
112	The seasonal cycle amplitude of total column CO2: Factors behind the model-observation mismatch. Journal of Geophysical Research, 2011, 116, n/a-n/a.	3.3	24
113	HIAPER Pole-to-Pole Observations (HIPPO): fine-grained, global-scale measurements of climatically important atmospheric gases and aerosols. Philosophical Transactions Series A, Mathematical, Physical, and Engineering Sciences, 2011, 369, 2073-2086.	1.6	351
114	Evaluation of methane emissions from West Siberian wetlands based on inverse modeling. Environmental Research Letters, 2011, 6, 035201.	2.2	39
115	Increasing synoptic scale variability in atmospheric CO <sub>2</sub> at Hateruma Island associated with increasing East-Asian emissions. Atmospheric Chemistry and Physics, 2010, 10, 453-462.	1.9	33
116	The Arabian Sea as a high-nutrient, low-chlorophyll region during the late Southwest Monsoon. Biogeosciences, 2010, 7, 2091-2100.	1.3	91
117	Long tails in deep columns of natural and anthropogenic tropospheric tracers. Geophysical Research Letters, 2010, 37, .	1.5	40
118	Stratospheric influence on the seasonal cycle of nitrous oxide in the troposphere as deduced from aircraft observations and model simulations. Journal of Geophysical Research, 2010, 115, .	3.3	43
119	Midâ€upper tropospheric methane in the high Northern Hemisphere: Spaceborne observations by AIRS, aircraft measurements, and model simulations. Journal of Geophysical Research, 2010, 115, .	3.3	44
120	Growth Rate, Seasonal, Synoptic, Diurnal Variations and Budget of Methane in the Lower Atmosphere. Journal of the Meteorological Society of Japan, 2009, 87, 635-663.	0.7	74
121	Formation mechanisms of latitudinal CO <sub>2</sub> gradients in the upper troposphere over the subtropics and tropics. Journal of Geophysical Research, 2009, 114, .	3.3	15
122	Transport mechanisms for synoptic, seasonal and interannual SF <sub>6</sub> variations and "age" of air in troposphere. Atmospheric Chemistry and Physics, 2009, 9, 1209-1225.	1.9	71
123	Condensedâ€phase flame retardation in nylon 6â€layered silicate nanocomposites: Films, fibers, and fabrics. Polymer Engineering and Science, 2008, 48, 662-675.	1.5	17
124	TransCom model simulations of hourly atmospheric CO <sub>2</sub> : Experimental overview and diurnal cycle results for 2002. Global Biogeochemical Cycles, 2008, 22, .	1.9	142
125	TransCom model simulations of hourly atmospheric CO <sub>2</sub> : Analysis of synopticâ€scale variations for the period 2002–2003. Global Biogeochemical Cycles, 2008, 22, .	1.9	119
126	Temporal and spatial variations of the atmospheric CO <sub>2</sub> concentration in China. Geophysical Research Letters, 2008, 35, .	1.5	29

#	Article	IF	CITATIONS
127	Globalâ€scale transport of carbon dioxide in the troposphere. Journal of Geophysical Research, 2008, 113, .	3.3	54
128	Atmospheric deposition and surface stratification as controls of contrasting chlorophyll abundance in the North Indian Ocean. Journal of Geophysical Research, 2007, 112, .	3.3	64
129	Exploring the sensitivity of interannual basin-scale air-sea CO2fluxes to variability in atmospheric dust deposition using ocean carbon cycle models and atmospheric CO2inversions. Journal of Geophysical Research, 2007, 112, .	3.3	10
130	Coupling between Land and Ocean Biospheres as Observed by Sea-viewing Wide Field-of-view Sensor (SeaWiFS). Scientific Online Letters on the Atmosphere, 2007, 3, 77-80.	0.6	1
131	Sensitivity of inverse estimation of annual mean CO2sources and sinks to ocean-only sites versus all-sites observational networks. Geophysical Research Letters, 2006, 33, .	1.5	40
132	The Indian summer monsoon rainfall: interplay of coupled dynamics, radiation and cloud microphysics. Atmospheric Chemistry and Physics, 2005, 5, 2181-2188.	1.9	48
133	Analysis of atmospheric CO2 growth rates at Mauna Loa using CO2 fluxes derived from an inverse model. Tellus, Series B: Chemical and Physical Meteorology, 2005, 57, 357-365.	0.8	34
134	Interannual and decadal changes in the sea-air CO2flux from atmospheric CO2inverse modeling. Global Biogeochemical Cycles, 2005, 19, n/a-n/a.	1.9	105
135	Role of biomass burning and climate anomalies for land-atmosphere carbon fluxes based on inverse modeling of atmospheric CO2. Global Biogeochemical Cycles, 2005, 19, .	1.9	101
136	Trends in methane and sulfur hexafluoride at a tropical coastal site, Thumba (8.6°N, 77.°E), in India. Atmospheric Environment, 2004, 38, 1145-1151.	1.9	10
137	Effect of recent observations on Asian CO2 flux estimates by transport model inversions. Tellus, Series B: Chemical and Physical Meteorology, 2003, 55, 522-529.	0.8	24
138	Sensitivity of optimal extension of CO2 observation networks to model transport. Tellus, Series B: Chemical and Physical Meteorology, 2003, 55, 498-511.	0.8	14
139	An evaluation of CO2observations with Solar Occultation FTS for Inclined-Orbit Satellite sensor for surface source inversion. Journal of Geophysical Research, 2003, 108, n/a-n/a.	3.3	41
140	Halogen Occultation Experiment (HALOE) and balloon-borne in situ measurements of methane in stratosphere and their relation to the quasi-biennial oscillation (QBO). Atmospheric Chemistry and Physics, 2003, 3, 1051-1062.	1.9	13
141	Comment on "Effects of Cosmic Rays on Atmospheric Chlorofluorocarbon Dissociation and Ozone Depletion― Physical Review Letters, 2002, 89, 219803; author reply 219804.	2.9	30
142	Nanocomposite Fibers. Materials Research Society Symposia Proceedings, 2002, 740, 1.	0.1	5
143	Incremental approach to the optimal network design for CO2surface source inversion. Geophysical Research Letters, 2002, 29, 97-1-97-4.	1.5	32
144	Nitrous oxide emissions from the Arabian Sea: A synthesis. Atmospheric Chemistry and Physics, 2001, 1, 61-71.	1.9	62

#	Article	IF	CITATIONS
145	Statistics of atmospheric correlations. Physical Review E, 2001, 64, 016102.	0.8	84
146	Chlorine partitioning in the stratosphere based on in situ measurements. Tellus, Series B: Chemical and Physical Meteorology, 2000, 52, 934-946.	0.8	4
147	Seasonal and spatial variability in N2O distribution in the Arabian Sea. Deep-Sea Research Part I: Oceanographic Research Papers, 1999, 46, 529-543.	0.6	21
148	Seasonal variability in distribution and fluxes of methane in the Arabian Sea. Journal of Geophysical Research, 1998, 103, 1167-1176.	3.3	39
149	Variabilities in the fluxes and annual emissions of nitrous oxide from the Arabian Sea. Global Biogeochemical Cycles, 1998, 12, 321-327.	1.9	18
150	Observed vertical profile of sulphur hexafluoride (SF6) and its atmospheric applications. Journal of Geophysical Research, 1997, 102, 8855-8859.	3.3	50
151	Variability of eddy diffusivity in the stratosphere deduced from vertical distributions of N2O and CFC-12. Journal of Atmospheric and Solar-Terrestrial Physics, 1997, 59, 1149-1157.	0.6	8
152	Vertical distribution of methyl bromide over Hyderabad, India. Tellus, Series B: Chemical and Physical Meteorology, 1994, 46, 373-377.	0.8	7
153	Vertical distribution of methyl bromide over Hyderabad, India. Tellus, Series B: Chemical and Physical Meteorology, 1994, 46, 373-377.	0.8	9